AFCRL-67-0501
SEPTEMBER 1967
PHYSICAL SCIENCES RESEARCH PAPERS, NO. 340

AIR FORCE CAMBRIDGE RESEARCH LABORATORIES
L. G. HANSCOM FIELD, BEDFORD, MASSACHUSETTS

Application of Geometrical Optics to the Design and Analysis of Microwave Antennas

F. SHEPPARD HOLT

OFFICE OF AEROSPACE RESEARCH
United States Air Force

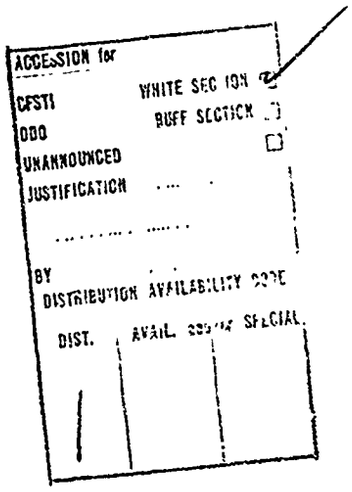

AFCRL-67-0501
SEPTEMBER 1967
PHYSICAL SCIENCES RESEARCH PAPERS, NO. 340

MICROWAVE PHYSICS LABORATORY PROJECT 5635

AIR FORCE CAMBRIDGE RESEARCH LABORATORIES

L. G. HANSCOM FIELD, BEDFORD, MASSACHUSETTS

Application of Geometrical Optics to the Design and Analysis of Microwave Antennas

F. SHEPPARD HOLT

OFFICE OF AEROSPACE RESEARCH

United States Air Force

Abstract

The basic concepts of geometrical optics together with the additional assumptions that lead to the "geometrical optics approximation" are described here. The eikonal equation is derived and the relationship of exact electromagnetic theory in the limit as $\lambda \to 0$ to geometrical optics is made evident. The application of the "geometrical optics approximation" to phase analysis and synthesis is described and an example of synthesis is presented. The concept of power flow in ray tubes is used to obtain approximations to power distributions in the antenna aperture, in the focal region, and in the far field. Ray analysis is used to determine those feed locations in the focal region that will most nearly collimate the far-field rays that lie in certain desirable planes. The Theorem of Malus is used to formulate the equal path length law and applications are given. Focal surfaces (or caustics) relative to a rectilinear congruence are defined and then used to present a geometrical optics description of the focal region. The equations of the focal surfaces of a paraboloid receiving a plane wave 20° off-axis are calculated and photographs of three-dimensional models of the focal surfaces are shown.

Contents

Illustrations

Application of Geometrical Optics to the Design and Analysis of Microwave Antennas

I. INTRODUCTION

This report is concerned with the laws, principles, and procedures of geometrical optics that are applicable to the design and analysis of microwave antennas. Geometrical optics, considered as a zero wavelength approximation to exact electromagnetic wave theory, is very accurate in the design and analysis of optical focusing devices because optical wavelengths are extremely small compared to the aperture dimensions of optical systems. At microwave frequencies, the wavelength is not always relatively small compared to the aperature dimensions of microwave systems. Geometrical optics, however, although certainly an approximation is still sufficiently accurate to produce meaningful and useful results, even for antennas with aperture dimensions as small as five wavelengths. The advantages of certain microwave components over existing optical components and the relaxation in mechanical tolerance requirements due to the finite wavelength allow the exploitation of geometrical optics analysis and design at microwave frequencies in certain cases considerably beyond that achievable in optics. For example, low-loss isotropic artificial dielectrics in a wide range of index of refraction, phase and amplitude control of sources and receivers, and aspheric as well as nonrotational symmetric reflecting and refracting surfaces are all available to the antenna designer.

(Received for publication 5 May 1967)

In general, geometrical optics is concerned with the analysis and synthesis of optical systems to the approximation that diffraction and interference can be neglected. In an isotropic medium, classical geometrical optics assumes that the power flows along paths called rays at a velocity characteristic of the medium and that there exists a family of surfaces known as wavefronts that are everywhere normal to the rays. Point-to-point correlation between wavefronts can be established by the rays and no power is assumed to be present in regions where there are no rays. It is evident, that if all the wavefronts are given, all the rays are determined and vice versa. Classical geometrical optics, therefore, neglects wavelength, phase, and the vector nature of electromagnetic wave motion. For microwave applications, it is most useful to extend the classical theory to include effects of the above-neglected factors. The form of the extension is justified by the asymptotic solution as $\omega \to \infty (\lambda \to 0)$ of the exact electromagnetic field equations to be discussed in Section 3. The extension consists of introducing wavelength as a small but finite quantity, identifying the wavefronts with equiphase surfaces, and at each point on a ray in a homogeneous medium introducing the electromagnetic field vectors $\underline{E}$ and $\underline{H}$ and relating them as in a plane wave propagating along the ray. We shall refer to this extension as the geometrical optics approximation.

2. THE EIKONAL AND THE EIKONAL EQUATION

Using the geometrical optics approximation, assume for a particular wave motion in a source-free isotropic medium that the equiphase wavefronts are given by the level surfaces of the function

$$L = L(x, y, z)$$

and that the phase ϕ on a general wavefront W is given by

$$\phi = \omega t - \frac{\omega}{c} L(x, y, z) \tag{1}$$

where ω is the angular frequency, c is the velocity in free space, and (x, y, z) is any point on W. The function $L(x, y, z)$ is known as the eikonal and, together with the wavefront velocity in the medium, it completely describes the given wave motion from the standpoint of classical geometrical optics.

Consider a general ray path C given by the equations

$$x = x(s)$$
$$y = y(s)$$
$$z = z(s) \qquad (2)$$

where s is arc length measured along C from a fixed reference wavefront W_o, given by $L(x, y, z) = 0$ to a propagating wavefront W (see Figure 1). Let the position of W along C as a function of time be given by the formula

$$s = s(t) \qquad (3)$$

where s increases with t. The wavefront propagation velocity v along C is then

$$v = \frac{ds}{dt} \quad . \qquad (4)$$

The value of $L(x, y, z)$ on the wavefront W will change as W propagates along C. Since time and position along C are related by (2) and (3), $L(x, y, z)$ may be considered as a function of either s or t. Thus

$$|\nabla L| = \frac{dL}{ds} = \frac{\frac{dL}{dt}}{\frac{ds}{dt}} \quad . \qquad (5)$$

Since the phase ϕ on the propagating wavefront W is constant, differentiating (1) with respect to t yields

$$\frac{d\phi}{dt} = \omega - \frac{\omega}{c}\frac{dL}{dt} = 0$$

or

$$\frac{dL}{dt} = c \, . \qquad (6)$$

Substituting (4) and (6) into (5) we have

$$|\nabla L| = \frac{c}{v} = n \qquad (7)$$

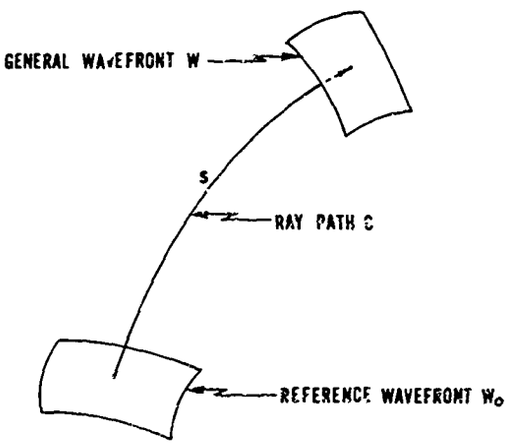

Figure 1. Ray Paths and Wavefronts

where n is the index of refraction of the medium. The partial differential equation (7) satisfied by the eikonal $L(x, y, z)$ is known as the eikonal equation.

The eikonal equation can be used to determine the curvature of ray paths in an inhomogeneous medium. Assume a wave motion in an inhomogeneous medium prescribed by the eikonal $L(x, y, z)$ and let C be a ray path with arc length s in the direction of the wave motion. At each point on C let $\underset{\sim}{\hat{s}}$ be the unit tangent vector in the direction of s, let $\underset{\sim}{\hat{n}}_p$ be the unit principal normal vector, and let ρ be the radius of curvature. The vector ∇L evaluated at any point P is normal to the wavefront passing through the point P. Hence, at each point on C, the vector ∇L is along C and in view of the eikonal equation (7),

$$\frac{\nabla L}{n} = \underset{\sim}{\hat{s}} \quad . \tag{8}$$

The first Frenet formula (Hildebrand, 1949) of differential geometry can be written

$$\frac{d\underset{\sim}{\hat{s}}}{ds} = (\underset{\sim}{\hat{s}} \cdot \nabla)\, \underset{\sim}{\hat{s}} = -\underset{\sim}{\hat{s}} \times (\nabla \times \underset{\sim}{\hat{s}}) = \frac{\underset{\sim}{\hat{n}}_p}{\rho} \quad . \tag{9}$$

Substituting (8) into (9) we have

$$\frac{d\underset{\sim}{\hat{s}}}{ds} = -\underset{\sim}{\hat{s}} \times \left[\nabla\left(\frac{1}{n}\right) \times \nabla L\right] = \underset{\sim}{\hat{s}} \times \left[\nabla(\ln n) \times \underset{\sim}{\hat{s}}\right]$$

and

$$\frac{1}{\rho} = \underset{\sim}{\hat{n}}_p \cdot \frac{d\underset{\sim}{\hat{s}}}{ds} = \underset{\sim}{\hat{n}}_p \cdot \nabla(\ln n) = \frac{1}{n}\, \underset{\sim}{\hat{n}}_p \cdot \nabla n \quad . \tag{10}$$

Equation (10) shows that the ray-path curvature $\frac{1}{\rho}$ is related to the rate of change of the index of refraction n normal to the ray path. In particular, for a homogeneous medium (n = constant) the curvature is zero and the ray paths are straight lines.

3. GEOMETRICAL OPTICS AS A ZERO WAVELENGTH APPROXIMATION

For a source-free nonconducting isotropic homogeneous medium, Maxwell's equations for the electric field $\underset{\sim}{E}$ and the magnetic field $\underset{\sim}{H}$ are

$$\nabla \times \underline{E} = -j\omega\mu \underline{H} \tag{11a}$$

$$\nabla \times \underline{H} = j\omega\epsilon \underline{E} \tag{11b}$$

$$\nabla \cdot \underline{E} = 0 \tag{11c}$$

$$\nabla \cdot \underline{H} = 0 \tag{11d}$$

where ω is the angular frequency, ϵ is the permittivity of the medium, μ is the permeability of the medium, and an $e^{j\omega t}$ time dependence is assumed. Equations (11a, b, c) combine to produce

$$\nabla^2 \underline{E} + k^2 \underline{E} = 0 \tag{12}$$

where $k = \omega\sqrt{\epsilon\mu}$ is the phase constant of the medium.

To obtain a zero wavelength or high frequency approximation, the electric field is assumed in the form of an asymptotic series (Luneberg, 1944; Kline and Kay, 1965; Kouyoumjian, 1965) in descending powers of ω as follows:

$$\underline{E}(x, y, z, \omega) = e^{-jk_o L(x, y, z)} \sum_{m=0}^{\infty} \frac{\underline{E}_m(x, y, z)}{(j\omega)^m} , \tag{13}$$

where $\underline{E}_o(x, y, z)$ is real and $k_o = \omega\sqrt{\epsilon_o\mu_o}$ is the phase constant of free space. Substituting (13) into (12) and independently equating to zero the coefficients of ω^2 and ω, the highest powers of ω present, yields

$$|\nabla L|^2 = n^2 \tag{14}$$

and

$$(\nabla L \cdot \nabla) \underline{E}_o + \frac{\nabla^2 L}{2} \underline{E}_o = 0 , \tag{15}$$

where $n = \frac{k}{k_o}$ is the index of refraction of the medium.

Note that (14) is the eikonal equation and hence $L(x, y, z)$ is the eikonal. As ω becomes large, the leading term of (13) predominates and becomes $\underline{E}_{HF}$, the high frequency approximation to the electric field, as follows:

$$\underline{E}_{HF} = \underline{E}_o(x, y, z) e^{-jk_o L(x, y, z)} . \tag{16}$$

Since $\underline{E}_o(x, y, z)$ is real, the equiphase surfaces $L(x, y, z) =$ constant of $\underline{E}_{HF}$ are identical with the wavefronts of geometrical optics. Again, the rays can be

defined as the family of curves normal to the wavefronts. In the present case of an isotropic homogeneous medium, the rays are straight lines (see Section 2).

At each point on a ray $\frac{\nabla L}{n} = \underline{s}$ is a unit vector tangent to the ray [see Eq. (8)]. Thus,

$$\nabla L \cdot \nabla = n \frac{\nabla L}{n} \cdot \nabla = n \underline{s} \cdot \nabla = n \frac{d}{ds} \tag{17}$$

where $\frac{d}{ds}$ is the directional derivative in the direction of a ray with respect to arc length s along the ray. Equation (15) can now be written

$$\frac{d\underline{E}_o}{ds} + \frac{1}{2} \frac{\nabla^2 L}{n} \underline{E}_o = 0 . \tag{18}$$

The solution to (18) along a ray through the point (x_o, y_o, z_o) can be expressed in the form

$$\underline{E}_o(s) = \underline{E}_o(s_o)\, e^{-\frac{i}{2}\int_{s_o}^{s} \frac{\nabla^2 L}{n}\, ds} \tag{19}$$

where s_o is the distance from a reference wavefront to the point (x_o, y_o, z_o). Thus, $\underline{E}_o(s)$ at any point on a ray is completely determined once its value is known at one point on the ray. This is a very clear statement of the geometrical optics property of point-to-point correlation from wavefront to wavefront along a ray. It is also evident from (19) that the direction of $\underline{E}_o$ is the same for all points on a ray (except possibly for sense).

Substituting (13) into (11c) and equating to zero the coefficient of ω^2, the highest power of ω, leads to the result

$$\nabla L \cdot \underline{E}_{HF} = 0 \tag{20}$$

and hence $\underline{E}_{HF}$ at each point on a ray is normal to the ray. Substituting (13) into (11a) and retaining only the highest order terms in ω yields $\underline{H}_{HF}$, the high frequency approximation to the magnetic field, as follows:

$$\underline{H}_{HF} = \frac{-jk_o}{-j\omega\mu} \nabla L \times \underline{E}_o\, e^{jk_o L} = \sqrt{\frac{\epsilon}{\mu}}\, \underline{s} \times \underline{E}_{HF} . \tag{21}$$

Equations (20) and (21) show that $\underline{E}_{HF}$ and $\underline{H}_{HF}$ along a ray are related precisely as in a plane wave propagating in the direction of the ray.

Simplification of (19) is best accomplished by considering the vector field

$$\underline{F} = Kn\,\underline{\hat{s}}\ ,\ K = \frac{1}{R_1 R_2} \tag{22}$$

where at each point R_1 and R_2 are the principal normal radii of curvature of the wavefront passing through that point (see Appendix A). The quantity $K = \frac{1}{R_1 R_2}$ evaluated at a point on a surface is known as the Gaussian curvature of the surface at that point. It can be shown that the surface integral

$$\iint_{\Sigma} \underline{F} \cdot d\underline{A} = 0 \tag{23}$$

where Σ is any closed surface lying in the isotropic homogeneous medium being considered. The divergence theorem then requires that

$$\nabla \cdot \underline{F} = 0$$

throughout the medium and hence

$$(n\,\underline{\hat{s}} \cdot \nabla)\,K = -K\,\nabla \cdot n\,\underline{\hat{s}} = -K\,\nabla^2 L\ .$$

in view of (17) it follows that

$$\frac{dK}{ds} + \left(\frac{\nabla^2 L}{n}\right)K = 0\ .$$

Hence,

$$\frac{K(s)}{K(s_o)} = e^{-\int_{s_o}^{s} \frac{\nabla^2 L}{n}\, ds}\ .$$

Equation (19) can now be written

$$\underline{E}_o(s) = \underline{E}_o(s_o)\sqrt{\frac{K(s)}{K(s_o)}}\ . \tag{24}$$

By applying (17) to the eikonal $L(x, y, z)$ and using (14) we have

$$\nabla L \cdot \nabla L = n^2 = n\frac{dL}{ds}$$

or

$$dL = nds .$$

For a homogeneous medium n is constant and

$$L = ns + L_o . \tag{25}$$

Substituting (24) and (25) into (16) yields

$$\underline{E}_{HF} = \underline{E}_o(s_o)\sqrt{\frac{K(s)}{K(s_o)}}\; e^{-jk_o L_o}\, e^{-jks} . \tag{26}$$

Note that the amplitude factor $\sqrt{\frac{K(s)}{K(s_o)}}$ is precisely equivalent to the geometrical optics power factor $\frac{K(d)}{K(0)}$ shown in (B3) of Appendix B.

4. FERMAT'S PRINCIPLE AND SNELL'S LAWS

The optical path length (OPL) along a ray path C is defined as the line integral $\int_C nds$ where n is the index of refraction of the medium and s is arc length along C. Fermat's principle states that electromagnetic energy traveling between two points will follow any ray path that makes the OPL integral stationary. Clearly then, ray paths in a homogeneous medium will be straight lines.

Snell's laws of reflection and refraction of rays at a boundary surface between two different media can be derived directly from Fermat's principle, but will merely be stated here. The law of reflection states that the incident ray and the reflected ray lie on the same side of the boundary surface, are coplanar with the normal to the boundary surface at the point of reflection, and make equal angles with the normal. Thus, $\theta_i = \theta_r$ where θ_i is the angle of incidence and θ_r is the angle of reflection, as shown in Figure 2. This reflection law can be expressed in any of the equivalent vector forms

$$\underline{\hat{n}} \times (\underline{\hat{s}}_r - \underline{\hat{s}}_i) = 0 , \tag{27a}$$

$$\underline{\hat{n}} \cdot (\underline{\hat{s}}_r + \underline{\hat{s}}_i) = 0 , \tag{27b}$$

$$\underline{\hat{s}}_r = \underline{\hat{s}}_i - 2(\underline{\hat{s}}_i \cdot \underline{\hat{n}})\,\underline{\hat{n}} , \tag{27c}$$

or

$$\underline{\hat{s}}_i = \underline{\hat{s}}_r - 2(\underline{\hat{s}}_r \cdot \underline{\hat{n}})\,\underline{\hat{n}} , \tag{27d}$$

where

$$\left|\underline{\hat{s}}_i\right| = \left|\underline{\hat{s}}_r\right| = \left|\underline{\hat{n}}\right| = 1 \tag{27e}$$

and $\underline{\hat{s}}_i$ is in the direction of the indicent ray, $\underline{\hat{s}}_r$ is in the direction of the reflected ray, and $\underline{\hat{n}}$ is normal to the boundary surface (see Figure 2).

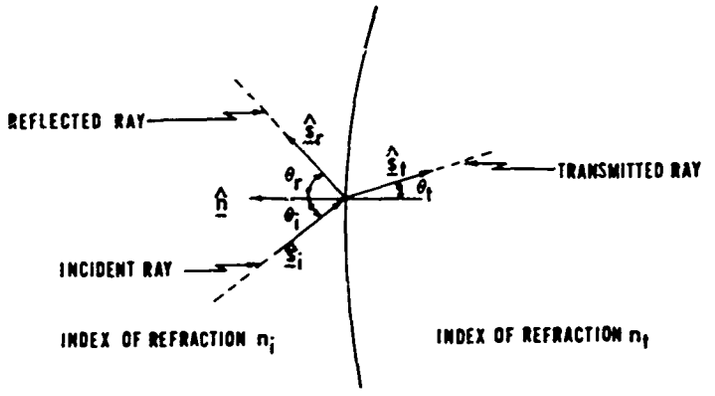

Figure 2. Reflection and Refraction at a Boundary

The law of refraction states that the incident ray and the transmitted or refracted ray lie on opposite sides of the boundary surface, are coplanar with the normal to the surface at the point of refraction, and satisfy the condition

$$n_i \sin\theta_i = n_t \sin\theta_t , \tag{28}$$

where n_i and n_t are the indices of refraction in the incident and transmitted regions respectively and θ_i and θ_t are the angles of incidence and refraction respectively (see Figure 2). This refraction law can be expressed in the vector form

$$\underline{\hat{n}} \times (n_i \underline{\hat{s}}_i - n_t \underline{\hat{s}}_t) = 0 \tag{29}$$

where $\underline{\hat{n}}$, $\underline{\hat{s}}_i$, n_i, and n_t are as defined above and $\underline{\hat{s}}_t$ is a unit vector in the direction of the transmitted ray.

Combining (27a) and (29), we have as a statement of both of Snell's laws

$$\underline{\hat{n}} \times n_i \underline{\hat{s}}_i = \underline{\hat{n}} \times n_r \underline{\hat{s}}_r = \hat{n} \times n_t \underline{\hat{s}}_t \tag{30}$$

where $n_r = n_i$, that is, the incident and reflected regions have the same index of refraction.

5. PHASE ANALYSIS AND PHASE SYNTHESIS

The geometrical optics approximation can be applied usefully to certain problems in phase analysis and phase synthesis. An application to phase synthesis is given in this section.

If $L(x, y, z)$ is the eikonal function, then, according to (1), the phase ϕ at a point P with coordinates (x, y, z) is

$$\phi = \omega t - \frac{\omega}{c} L(x, y, z) .$$

If W_o is the wavefront $L(x, y, z) = 0$ then the phase ϕ_o over the whole wavefront W_o is

$$\phi_o = \omega t .$$

The phase at P relative to the phase on W_o, that is, the phase difference ϕ_Δ between P and W_o, will be

$$\phi_\Delta = \phi - \phi_o = -\frac{\omega}{c} L(x, y, z) . \tag{31}$$

Assuming that the ray through P intersects W_o at point P_o, then, according to Section 4, the optical path length from P to P_o is defined as

$$\text{OPL} = \int_{P_o}^{P} n\,ds ,$$

where n is the index of refraction of the medium and the path of integration is along the ray from P_o to P. The phase difference ϕ_Δ between P and P_o can be expressed in terms of OPL as follows:

$$\phi_\Delta = -\frac{2\pi}{\lambda_o} \int_{P_o}^{P} n\,ds , \tag{32}$$

where λ_o is the free-space wavelength. Noting that $\frac{\omega}{c} = \frac{2\pi}{\lambda_o}$ and comparing (31) with (32), it is evident that the eikonal function $L(x, y, z)$ evaluated at P is equal to the OPL from the reference wavefront to P. The geometrical optics determination of phase will clearly fail in any region where two or more rays pass through each point.

Now consider the problem of designing a point-source-fed reflector in two dimensions in a medium of index n that will synthesize to within the geometrical optics

approximation a given phase distribution along a line (Sletten, 1958). Let the point source be located at the point F with coordinates (0, a) and let the x axis be the line along which it is desired to achieve the phase function f (x) . If a ray reflected from the reflector at the point P with coordinates (x, y) intersects the x axis at the point P_o with coordinates (x_o , 0), as shown in Figure 3, then it follows from (32) that

$$\left(\frac{2\pi}{\lambda}\right)n\ \sqrt{x^2 + (y-a)^2} + \left(\frac{2\pi}{\lambda}\right)\ n\ \sqrt{(x-x_o)^2 + y^2}\ = -f(x_o) + C_1 \qquad (33)$$

where C_1 is a constant that can be adjusted to control the position of the reflector and the extent of useable aperture. For x_o fixed (33) as a function of x and y represents an ellipse with foci at F and P_o . With x_o variable (33) represents a one parameter family of ellipses that, in general, has an envelope. To each ellipse in the family there corresponds a unique point on the envelope where the ellipse is a tangent to the envelope. By using the envelope as the reflector surface, it is clear that at each point on the envelope the incident ray is precisely reflected, as from the ellipse corresponding to that point, and hence arrives at the x axis in proper phase.

The envelope of the family of ellipses is given by the simultaneous solution of (33) with the partial derivative of (33) with respect to x_o , that is,

$$\frac{2\pi n}{\lambda}\ \frac{(x - x_o)}{\sqrt{(x-x_o)^2 + y^2}}\ = f'(x_o)\ . \qquad (34)$$

Carrying out the simultaneous solution of (33) and (34) leads to the result

$$x = x_o + \frac{B}{2}\left[\frac{(A^2 + x_o^2 - a^2)}{(Bx_o + A + a\sqrt{1-B^2})}\right]$$

$$y = \frac{1-B^2}{2}\left[\frac{(A^2 + x_o^2 - a^2)}{(Bx_o + A + a\sqrt{1-B^2})}\right] \qquad (35)$$

where

$$A = \frac{\lambda}{2\pi n}\ \left[C_1 - f(x_o)\right]$$

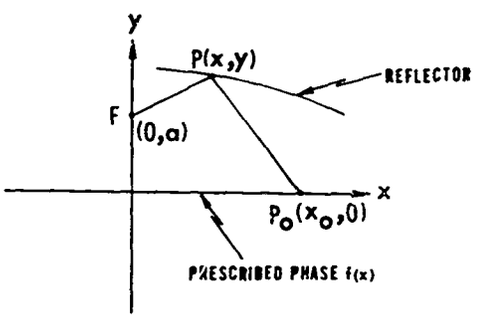

Figure 3. Geometry of Reflector to Produce Desired Phase Along a Line

and

$$B = \frac{\lambda}{2\pi n} f'(x_o) .$$

An experimental line source feed designed by the above procedure for off-focus feeding of a paraboloid, was very successful in producing a well-focused off-axis fan beam.

6. POWER FLOW IN RAY TUBES

One of the important assumptions of geometrical optics is that the power flows along the ray paths. Therefore, a ray path diagram presents an overall picture of the power flow for a lossless source-free medium to within the accuracy of this approximation. The totality of rays that pass through any given closed curve constitutes a ray tube; and, under steady state conditions, the total power flowing across any cross section of a ray tube must be constant since no power can flow across the lateral surfaces of the tube. Thus, as a ray tube cross section decreases the power density increases and, conversely, as a ray tube cross section increases the power density decreases. These two cases correspond to converging and diverging rays respectively. In particular, if dA is a differential area on a wavefront W and if the ray tube passing through dA intersects the wavefront W' in the differential area dA' (see Figure 4), then, the total power flow through dA must equal the total power flow through dA'. Thus, we have

$$P\,dA = P'\,dA' \tag{36}$$

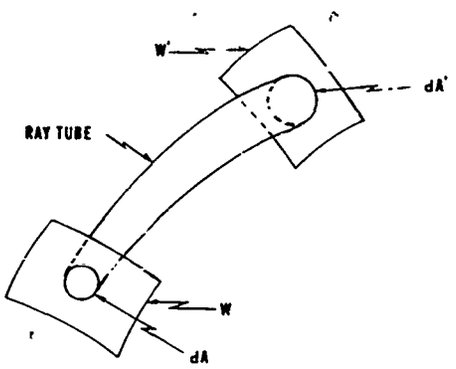

Figure 4. A Ray Tube Between Wavefronts

where P is the power density at dA and P' is the power density at dA'. It is clear that the ray tube concept of power flow will break down at focal points since at such points the ray tube cross section vanishes and (36) predicts infinite power density.

The concept of power flowing in ray tubes as applied to the region between the primary-feed and the aperture is particularly useful in the design and analysis of antennas. In far-field considerations, it is also useful in the design and/or analysis of certain shaped

beam and off-focus-fed antenna systems. The ray tube concept finds little application in far-field considerations relative to well-focused pencil beam systems since in such cases the pattern is determined entirely by diffraction.

7. POWER DISTRIBUTION IN THE APERATURE

In using geometrical optics to investigate antenna aperture-plane power distributions or to design primary feeds for optimum illumination, the important quantity furnished by the ray tube concept is an approximation to the relative power distribution.

To determine the relative power distribution, it is necessary to know the absolute power distribution to within only an arbitrary multiplicative constant. Hence, if either the absolute or the relative power distribution is known on a wavefront W (see Figure 4), then, in using (36) in the form

$$P' = \frac{dA}{dA'} P \tag{37}$$

to determine the geometrical optics approximation to the relative power distribution on W', it is necessary to know $\frac{dA}{dA'}$ to within only a multiplicative constant.

For a well-focused, point-source-fed antenna system, the usual procedure for determining the geometrical optics approximation to the relative power distribution on the antenna aperture plane for a given primary feed power pattern is to first analyze the system when fed by an isotropic point source. All wavefronts will be spheres for the isotropic feed and the power density will be constant over any fixed wavefront W. Also, any differential element of area dA on the wavefront W will be proportional to the differential solid angle $d\Omega$ subtended by dA as measured at the feed. A general ray trace of the antenna system will determine the aperture coordinates of the exit ray, as functions of the ray direction coordinates, as measured at the feed. These relations will determine the area dA' in the aperture plane W' (assumed to coincide with a wavefront) that corresponds to the differential element of area dA in the wavefront W. Since $d\Omega = KdA$, where K is a constant, the quantity $\frac{d\Omega}{dA'}$ is proportional to $\frac{dA}{dA'}$ and can therefore be used in the calculation of the relative power distribution on W'. If the primary feed has a relative power pattern $P(\theta, \phi)$, where θ and ϕ are the ray direction coordinates, then the geometrical optics approximation to the relative power distribution on the aperture plane is proportional to $P(\theta, \phi) \frac{d\Omega}{dA}$, where (in theory) θ and ϕ can be expressed in terms of the aperture coordinates.

The geometrical optics approximation to the relative power distribution on the aperture of a well-focused, line-source-fed cylindrical antenna system can be

determined by procedures analogous to those used for the point-source case. It will be assumed that the relative power pattern of the line-source feed is of the form $P(\theta, z) = g_1(\theta)g_2(z)$, where z is the linear coordinate parallel to the feed line and θ is the angular coordinate around the feed. Since the antenna system is cylindrical, all rays from any one point on the feed line remain in a plane normal to the feed line and, in all such planes, ray trace diagrams are identical. Thus, power will only flow parallel to these planes and the identity of the ray trace diagrams guarantees that the relative power distribution on the aperture plane in the z direction will be proportional to $g_2(z)$. This reduces the problem by one dimension and leads to the consideration of the power flow in a typical plane normal to the feed line. For a feed isotropic in θ, the wavefronts are circles and the power density on these circles is uniform. If ds is a differential element of arc length on a fixed wavefront C and if $d\theta$ is the differential angle at the feed subtended by ds, then, since C is a circle, it follows that ds is proportional to $d\theta$. A general ray trace will relate θ to h, where h is the exit ray aperture coordinate normal to z; this relation will determine the differential element dh in the aperture plane (assumed coincident with a wavefront) that corresponds to ds. Since $ds = K' d\theta$ where K' is a constant, it follows that $\frac{d\theta}{dh}$ is proportional to $\frac{ds}{dh}$ and can therefore be used in the calculation of the relative power distribution on the aperture plane with respect to the h coordinate. For the given feed with relative power pattern $P(\theta, z) = g_1(\theta)g_2(z)$, the geometrical optics approximation to the relative power distribution on the aperture plane is proportional to $g_1(\theta)g_2(z)\frac{d\theta}{dh}$, where (in theory) θ can be expressed in terms of h.

As a simple example of this procedure applied to a cylindrical system, consider a parabolic cylinder reflector of focal length f with its focal line coincident with the z axis. Figure 5 shows a central plane section of this reflector with polar coordinates (r, θ) describing the reflector surface and the linear coordinate h designating position in the aperture plane $x = 0$. The equation of the reflector surface in (r, θ) coordinates is

$$r = \frac{2f}{1 + \cos\theta} = f \sec^2(\theta/2).$$

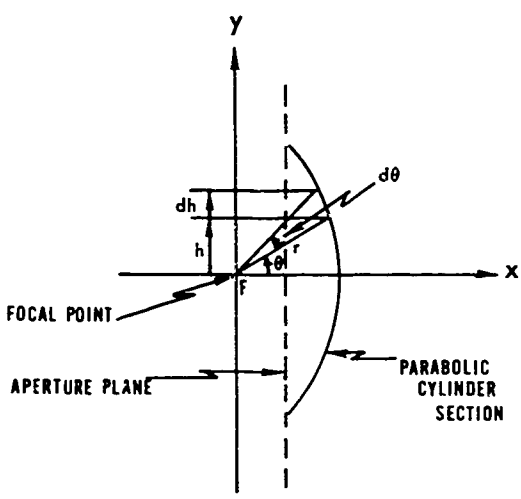

Figure 5. Central Plane Section of a Parabolic Cylinder Antenna

The primary feed located at F (see Figure 5) is assumed to radiate uniformly in θ and all rays originating at F are assumed to be reflected

parallel to and in the direction of the negative x axis. Thus,

$$h = r \sin\theta = 2f \tan(\theta/2)$$

$$dh = f \sec^2(\theta/2)d\theta = rd\theta \quad .$$

and

$$\frac{d\theta}{dh} = \frac{1}{r} \quad .$$

If the given primary feed has a power pattern $P(\theta, z) = g_1(\theta)g_2(z)$, then, P_a, the geometrical optics approximation to the relative power distribution on the aperture normalized at the center of the aperture, is given by

$$P_a = \frac{f}{r} \frac{g_1(\theta)g_2(z)}{g_1(0)g_2(0)} \quad . \tag{38}$$

This is certainly a correct result from the geometrical optics standpoint since it clearly demonstrates that the power spreads radially, that is, inversely proportional to distance, only in planes normal to the feed line and only over the distance from the feed to the reflector, that is, over the distance r. After reflection, the rays are collimated and no more spreading takes place out to the aperture plane.

8. POWER DISTRIBUTION IN THE FOCAL REGION

In the analysis of an imperfectly-focused antenna such as a spherical reflector or an off-axis-fed paraboloid, it is frequently desired to obtain an estimate of the relative power distribution along some focal surface or curve in the focal region. In this case, the ratio of a differential element of surface area of the incoming plane wavefront to the corresponding differential element of surface area or arc length in the focal region is an estimate of the relative power distribution on the appropriate focal surface or curve.

Consider, for example, the problem of determining the power distribution along the axis of a spherical reflector of radius "a" illuminated by a plane wave incident along the axial direction (see Figure 6). By symmetry all rays after reflection pass through the reflector axis. The height h of an incident ray and the coordinate z of the intersection of the corresponding reflected ray with the reflector axis are related to the angle θ as follows:

$$h = a \sin\theta$$

and

$$z = \frac{a}{2\cos\theta} .$$

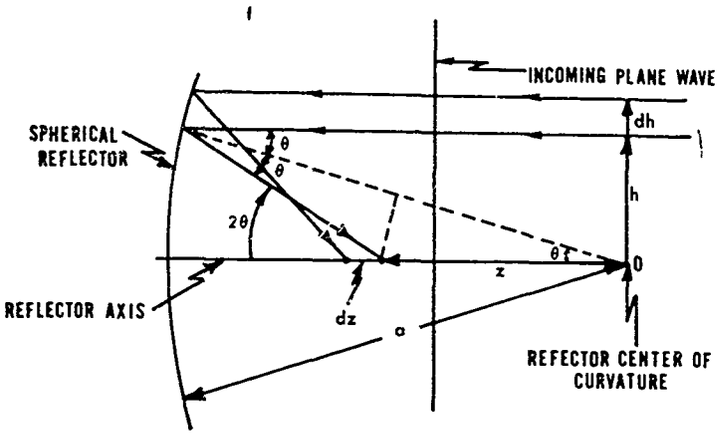

Figure 6. Central Section of a Spherical Reflector

Hence,

$$h^2 = a^2 \left(1 - \frac{a^2}{4z^2}\right) . \tag{39}$$

The differential area dA generated by revolving the line segment dh about the reflector axis is

$$dA = 2\pi h\, dh .$$

All incident rays passing through dA will, after reflection, pass through the differential line element dz. Thus, the power distribution P along the reflector axis is

$$P = B\frac{dA}{dz} = 2\pi hB\frac{dh}{dz} \tag{40}$$

where B is a constant. From (39) we have

$$2h \frac{dh}{dz} = \frac{a^4}{2z^3}$$

and (40) becomes

$$P = \frac{\pi B a^4}{2z^3} .$$

From (39) we have

$$\lim_{h \to 0} z = a/2 . \tag{41}$$

This is known as the paraxial focus point. Normalizing the power distribution to unity at the paraxial focus point the relative power distribution P_r along the reflector becomes

$$P_r = \frac{a^3}{8z^3} .$$

9. POWER DISTRIBUTION IN THE FAR FIELD

In the use of the ray tube concept to approximate antenna far-field power patterns, the underlying assumption is that the radiated power after it leaves the final surface of the antenna flows along ray tubes not only up to the aperture plane but indeed on out into the antenna far field. This assumption is clearly invalid for well-focused antenna systems, that is, for systems all of whose exit rays are nearly parallel, since in such cases the pattern is determined entirely by diffraction. However, for systems that are not well-focussed in one or in both planes, the ray tube concept provides a useful approximation to the relative far-field pattern. In any plane in which the exit rays are not parallel, the power flow per unit directional angle or per unit solid angle in the exit ray system is determined by the ray-tube concept as a function of angular direction; this function, after appropriate normalization, is the geometrical optics approximation to the far-field antenna pattern.

As an example of the use of this far-field approximation, consider the design of a line-source fed cylindrical reflector to produce a fan beam of prescribed shape (Spencer, 1943). Let S be the plane of symmetry of this antenna normal to the line source. The cylindrical geometry guarantees that all exit rays lying in planes normal to S are parallel and therefore S will be the plane of the fan

beam. It is desired to determine the shape of the reflector cross section that will cause ray dispersion in the plane of S appropriate to produce the prescribed fan beam shape. It is assumed that the primary feed pattern $P_f(\theta)$ and the desired secondary power pattern $P(\phi)$ are given. The angles θ and ϕ are measured positive clockwise in the plane of S. (See Figure 7a.) For practical purposes, the useful portion of the primary feed pattern $P_f(\theta)$ lies between its -10 dB points and will be designated by the interval $\theta_1 \leq \theta \leq \theta_2$. Generally, the function $P(\phi)$ vanishes everywhere except within some interval, say $\phi_1 \leq \phi \leq \phi_2$, where it takes on a prescribed form. Thus, rays from the line-feed incident on the reflector with inclination angle θ, $\theta_1 \leq \theta \leq \theta_2$ must produce reflected rays with inclination angle ϕ, $\phi_1 \leq \phi \leq \phi_2$ (see Figure 7a).

The problem now is to determine a one-to-one correspondence between the incident and reflected rays—that is, a function $\phi = \phi(\theta)$ such that the reflected ray system has a power distribution corresponding to $P(\phi)$. In a differential sector $d\theta$ of the incident ray system, the power flow is proportional to $P_f(\theta)d\theta$; in a corresponding differential sector $d\phi$ of the reflected ray system, the power flow is proportional to $P(\phi)\, d\phi$. Thus,

$$P_f(\theta)\, d\theta = KP(\phi)\, d\phi$$

where K is determined by the relation

$$\int_{\theta_1}^{\theta_2} P_f(\theta)\, d\theta = K \int_{\phi_1}^{\phi_2} P(\phi)\, d\phi,$$

which is equivalent to requiring equal total powers in the incident and reflected ray systems. We also require the power in the incident ray system in the interval θ_1 to θ to be equal to the power in the reflected ray system in the interval ϕ_1 to ϕ. Thus,

$$\frac{\int_{\theta_1}^{\theta} P_f(\theta)\, d\theta}{\int_{\theta_1}^{\theta_2} P_f(\theta)\, d\theta} = \frac{\int_{\phi_1}^{\phi} P(\phi)\, d\phi}{\int_{\phi_1}^{\phi_2} P(\phi)\, d\phi} \tag{42}$$

and this expression determines the required relationship $\phi = \phi(\theta)$.

We now turn to the determination of the equation for the reflector curve. With the reflector curve denoted by $r = r(\theta)$ we have from Figure 7b

$$\tan \psi = \frac{r d\theta}{dr}$$

and

$$\psi = \frac{\pi}{2} + \beta = \frac{\pi}{2} + \frac{\phi - \theta}{2} \quad .$$

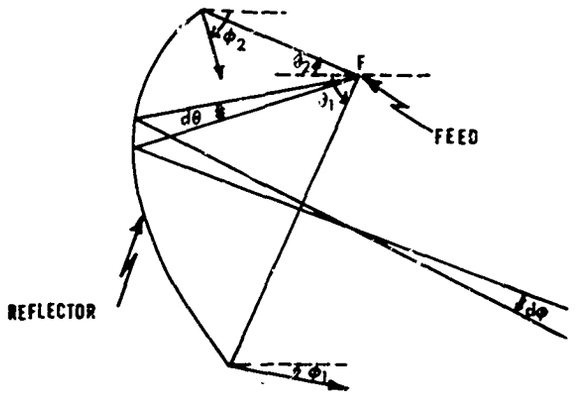

Figure 7a

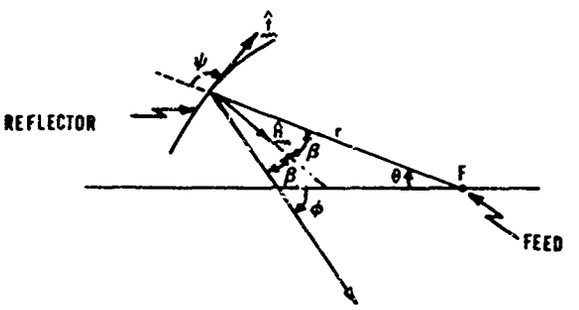

Figure 7b

Figure 7. Shaped-Beam Reflector Geometry in the Plane of Symmetry S

Thus,

$$\frac{1}{r}\,dr = \cot\left(\frac{\theta - \phi}{2}\right) d\theta = \cot\left[\frac{\theta - \phi(\theta)}{2}\right] d\theta$$

or

$$\ln\left(\frac{r}{r_o}\right) = \int_o^\theta \cot\left[\frac{\theta - \phi(\theta)}{2}\right] dB\ , \tag{43}$$

where

$$r_o = r(0)\ .$$

Equation (43) determines the desired reflector curve to within a radial scale factor r_o. Overall physical dimensions, as well as the requirement that the reflector be in the far field of the feed, establish a range of permissible values for r_o.

Generally, the function $P_f(\theta)$ is given graphically while $P(\phi)$ may be given analytically, graphically, or numerically. Therefore, in most cases numerical integration will be required to determine $\phi = \phi(\theta)$ from (42) and the resultant relationship will be expressed in numerical form. Numerical integration will be required to solve (43) for the reflector curve $r = r(\theta)$.

10. REFLECTION FROM A CONDUCTING SURFACE

In an isotropic homogeneous medium, the geometrical optics approximation assumes that the energy propagates along the rays as in a plane wave. To within this approximation, therefore, the field vectors $\underline{E}$ and $\underline{H}$ along a ray are related as follows:

$$\underline{H} = \sqrt{\frac{\epsilon}{\mu}}\ \underline{\hat{s}} \times \underline{E} \tag{44a}$$

$$\underline{S} = \underline{E} \times \underline{H}^* = \sqrt{\frac{\epsilon}{\mu}}\ |\underline{E}|^2\ \underline{\hat{s}} \tag{44b}$$

$$\underline{\hat{s}} \cdot \underline{E} = \underline{\hat{s}} \cdot \underline{H} = \underline{E} \cdot \underline{H} = 0 \tag{44c}$$

where $\underline{S}$ is the Poynting vector and $\underline{\hat{s}}$ is a unit vector in the direction of the ray (see Figure 8). The magnitude of $\underline{E}$ (and hence of $\underline{H}$ and $\underline{S}$) is prescribed by (24).

With the above assumptions, consider reflection from a smooth, perfectly-conducting surface V. Let $\underline{E}_i$ be the electric field incident on V along the ray direction $\underline{\hat{s}}_i$, let $\underline{E}_r$ be the electric field reflected from V along the corresponding ray direction $\underline{\hat{s}}_r$, and let $\underline{\hat{n}}$ be the unit surface normal to V (see Figure 9).

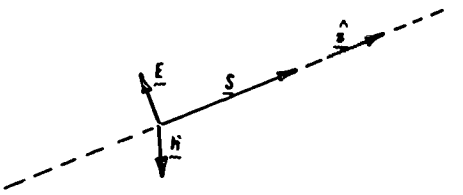

Figure 8. Electric and Magnetic Fields Along a Ray Path

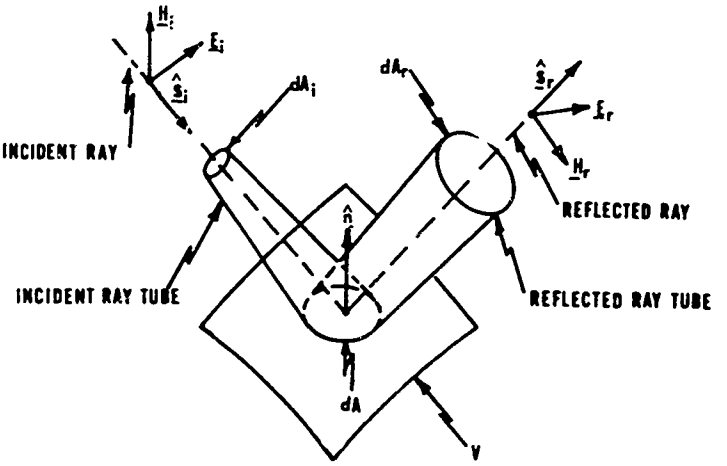

Figure 9. Incident and Reflected Electromagnetic Fields and Ray Tubes

Consider a differential area dA on V. Let dA_i be the differential cross section of the ray tube incident on dA and let dA_r be the differential cross section of the ray tube reflected from dA. Evaluating dA_i and dA_r at V, we have the following relations:

$$dA = \frac{dA_i}{|\underline{\hat{n}} \cdot \underline{\hat{s}}_i|} = \frac{dA_r}{|\underline{\hat{n}} \cdot \underline{\hat{s}}_r|} .$$

Since Snell's law, (27b) gives

$$|\underline{\hat{n}} \cdot \underline{\hat{s}}_i| = |\underline{\hat{n}} \cdot \underline{\hat{s}}_r| ,$$

we have

$$dA_i = dA_r$$

and hence at V

$$|\underline{E}_i| = |\underline{E}_r| . \tag{45}$$

The continuity of the tangential electric field at the surface V requires

$$\hat{\underline{n}} \times (\underline{E}_i + \underline{E}_r) = 0 \tag{46}$$

and the plane wave assumption requires

$$\hat{\underline{s}}_i \cdot \underline{E}_i = \hat{\underline{s}}_r \cdot \underline{E}_r = 0 . \tag{47}$$

It follows from (45) and (46) that at V

$$\hat{\underline{n}} \cdot (\underline{E}_i - \underline{E}_r) = 0 \tag{48}$$

and

$$\underline{E}_r = 2 (\hat{\underline{n}} \cdot \underline{E}_i) \hat{\underline{n}} - \underline{E}_i \tag{49a}$$

or

$$\underline{E}_r = (\hat{\underline{n}} \cdot \underline{E}_i) \hat{\underline{n}} - \hat{\underline{n}} \times (\underline{E}_i \times \hat{\underline{n}}) . \tag{49b}$$

The magnetic fields $\underline{H}_i$ and $\underline{H}_r$ at V are given by (44a) and (49a) or (49b).

The above results show that, under the assumptions made, the reflection process locally at each point of V is equivalent to plane-wave reflection from an infinite conducting plane tangent to V at the point (Silver, 1949). The assumptions of plane-wave propagation along rays and local reflection behavior as from an infinite plane lead to useful approximations of the polarization characteristics of reflector-type antennas.

11. RAY COLLIMATION AND OFF-FOCUS FEEDING

Consider a focusing system fed by a point source not necessarily located at a focus point and let $\hat{\underline{s}}_r$ be a unit vector in the direction of the general exit ray.

The components of $\underline{s}_r$ will be the direction cosines of the exit rays, that is,

$$\underline{s}_r = \cos\alpha\ \underline{\hat{x}} + \cos\beta\ \underline{\hat{y}} + \cos\gamma\ \underline{\hat{z}}\ . \quad (49)$$

A different set of exit rays and associated direction cosines is generated for each different feed position. If the direction cosines are considered as functions of coordinates u and v that designate the rays--for instance, exit aperture coordinates--then total collimation of the rays is characterized by the conditions

$$\frac{\partial \cos\alpha}{\partial u} = \frac{\partial \cos\beta}{\partial u} = \frac{\partial \cos\gamma}{\partial u} = 0 \quad (50a)$$

and

$$\frac{\partial \cos\alpha}{\partial v} = \frac{\partial \cos\beta}{\partial v} = \frac{\partial \cos\gamma}{\partial v} = 0\ . \quad (50b)$$

All exit rays are totally collimated and the above conditions hold for all u and v in the on-focus case for a perfectly focusing system. Overall total collimation does not occur in the off-focus case; but, there may be conditions under which partial collimation is achieved for certain families of rays. Rays will be considered to be partially collimated if they are all parallel to the same plane; rays that are all parallel to two nonparallel planes will be totally collimated. Requiring any one of the direction cosines to vanish will determine conditions for partial collimation relative to one of the coordinate planes; for instance, setting $\cos\alpha = 0$ will determine for each different feed position the rays that are parallel to the plane $\alpha = \pi/2$, that is, the yz plane. The location of these partially-collimated rays is particularly important in antenna design, as it determines those portions of the focusing system that are the most effective in achieving partial collimation.

In practice, most focusing systems have a plane of symmetry U and all rays leaving the feed in U will remain in U. Therefore, these rays are partially collimated. If U is taken to be the yz coordinate plane, as shown in Figure 10, each ray in U can be designated by the angle θ at which it leaves the feed point $(0, y_o, z_o)$.

Applying the geometrical optics concepts of power flow in the far field as described in Section 9 to the two-dimensional case of the rays in U, the power density P per unit angle ϕ at a range R is given by the expression

$$P = \frac{K\,G(\theta)}{R\frac{d\phi}{d\theta}} \quad (51)$$

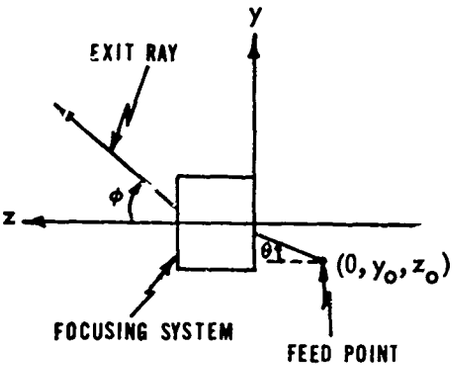

Figure 10. Section of Focusing System in the Plane of Symmetry U

where K is a constant and $G(\theta)$ is the feed power pattern in U. This expression gives a rough estimate of the far-field power pattern in the plane of U, provided $\frac{d\phi}{d\theta} \neq 0$. If the exit ray at angle $\phi = \phi_o$ corresponds to the ray leaving the feed at angle $\theta = \theta_o$, the condition

$$\left.\frac{d\phi}{d\theta}\right|_{\theta=\theta_o} = 0 \qquad (52)$$

determines the feed position that will produce local collimation of the rays in U that are in the neighborhood of the exit ray in the direction $\phi = \phi_o$. Under these conditions, geometrical optics predicts an infinite singularlity in the far-field pattern, which may be interpreted as a power pattern maximum in the direction $\phi = \phi_o$; but, relative magnitudes obviously cannot be determined without the use of diffraction.

12. CONGRUENCES AND THE EQUAL PATH LENGTH LAW

A two-parameter family of curves constitutes what is known in differential geometry as a congruence. The member curves of a congruence are called generators. If these generators are straight lines, the congruence is denoted as rectilinear. Furthermore, if there exists a surface that is normal to all the generators, the congruence is designated as normal. Thus, in a homogeneous isotropic medium, the normals to a wavefront—that is, the rays themselves—constitute a normal rectilinear congruence. It can also be shown that a normal rectilinear congruence possesses not just one normal surface but a whole family of normal surfaces (Eisenhart, 1960, p. 393); these surfaces, of course, correspond to wavefronts of the corresponding ray congruence.

Rectilinear congruences are not necessarily normal and, therefore, the Theorem of Malus (Eisenhart, 1960, p. 403) is of fundamental importance in ray-path analysis. This theorem states that if a family of rays, initially a normal rectilinear congruence, is reflected or refracted any number of times by successive homogeneous isotropic media, the rays will continue to constitute a normal rectilinear congruence. Therefore, for antenna systems satisfying the conditions of this theorem, both incident and exit wavefronts are guaranteed to exist. Since wavefronts are equiphase surfaces, it follows that between any two specific wavefronts the optical path lengths along all ray paths must be equal; this is a most important result and forms

the basis of the equal path length law and the associated design procedures applicable to reflection and refraction.

Consider the problem of designing a reflector R passing through a given point P_o that will reflect a given incident wavefront W into a desired reflected wavefront W' (see Figure 11). The desired reflector surface is given by the locus of points P determined by the condition

$$d + d' = d_o + d'_o \quad . \tag{53}$$

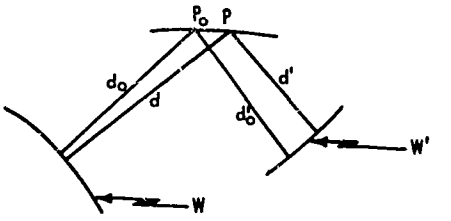

Figure 11. Wavefronts and Rays for Reflection From a Curved Surface

It is very important to note here that Snell's law of reflection will automatically be satisfied at the reflector surface. In the corresponding refraction problem, it is desired to determine the boundary surface S between two different homogeneous media passing through a given point P_o such that a given incident wavefront W is converted into a desired refracted wavefront W' (see Figure 12). In this case, the surface S is the locus of points P determined by the condition

$$nd + n'd' = nd_o + n'd'_o \quad , \tag{54}$$

and Snell's law of refraction will automatically be satisfied at the interface.

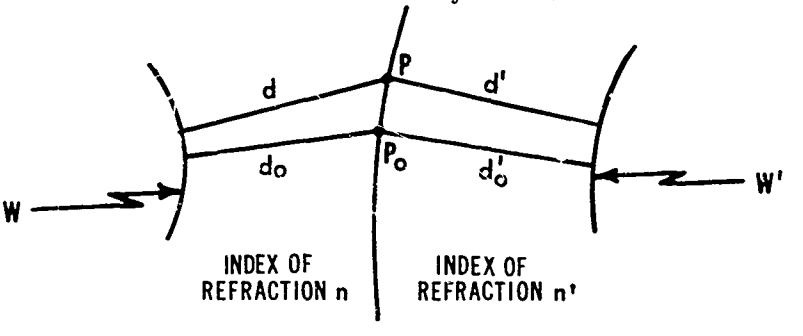

Figure 12. Wavefronts and Rays for Refraction Through a Curved Interface

In both of the above-mentioned procedures, it is necessary that the reflecting or refracting surface be located in a region where through each point there passes not more than one ray of the incident ray congruence and not more than one ray of the reflected or refracted ray congruence. If this restriction is violated, it will

not be possible to design a reflecting or refracting surface that satisfies the equal path length requirement along all rays.

As an example of the application of the equal path length law, consider the design of a reflector to correct for the inherent spherical aberration of a spherical reflector (Holt and Bouche, 1964). Let the radius of curvature of the spherical reflector be "a" and let the center of curvature be the origin. With the x axis as the reflector axis, an incoming plane wave along the x axis is assumed; the yz plane is the reference wavefront. The spherical reflector, the corrector, and the associated ray system are all radially symmetric about the reflector axis; therefore, all sections in planes through the x axis are the same (see Figure 13).

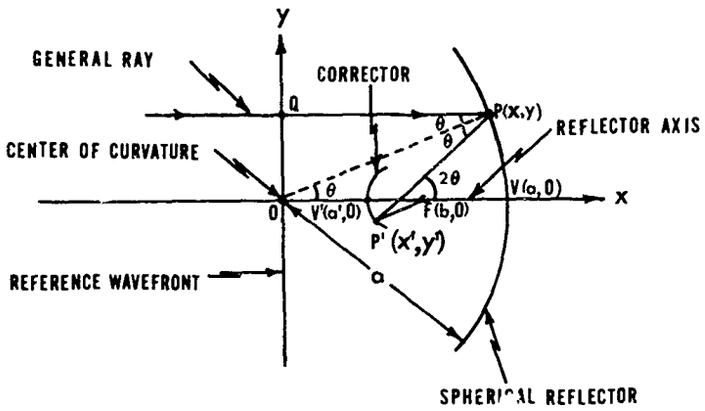

Figure 13. Spherical Reflector Section in the xy Plane

To fix the solution, let V with coordinates (a, 0) be the vertex of the reflector, let V' with coordinates (a', 0), $a' \leq a/2$, be the vertex of the corrector, and let F with coordinates (b, 0), $b > a'$, be the final focus point. The condition $a' \leq a/2$ guarantees that the corrector will lie in a region where only one ray of the incident ray congruence and only one ray of the reflected ray congruence will pass through each point.

Applying the equal path length law to the general ray QPP'F and the axial ray OVV'F, we have

$$\overline{QP} + \overline{PP'} + \overline{P'F} = \overline{OV} + \overline{VV'} + \overline{V'F}$$

or

$$a(\cos\theta) + \sqrt{(x' - x)^2 + (y' - y)^2} + \sqrt{(x' - b)^2 + y'^2} = 2a + b - 2a'$$

where

$$x = a\cos\theta\ ,\quad y = a\sin\theta\ ,\quad \text{and}\quad y' - y = (x' - x)\tan 2\theta\ .$$

Solving for x' and y', we obtain

$$x' = a\cos\theta - \frac{[a^2\cos^2\theta - 4a(a-a')\cos\theta - (a^2 + b^2) + (2a + b - 2a')^2]\,(2\cos^2\theta - 1)}{4(b\cos^2\theta - a\cos\theta - a' + a)} \tag{55a}$$

$$y' = \pm\ \frac{(2x'\cos\theta - a)(\sin\theta)}{(2\cos^2\theta - 1)} \tag{55b}$$

These are the coordinates of the corrector surface in terms of the parameter θ. Provided a' and b lie in the indicated ranges, the answer given above is valid and unique. (The $\pm$ sign for the y' value merely indicates symmetry with respect to the x axis.)

13. FOCAL SURFACES

Let us consider a wavefront W and its associated ray congruence. Let P be a point on W and let PN be a line segment normal to W (see Figure 14). If C_{R_1} is a line of curvature of W with $\rho = R_1$ at P (see Appendix A), then in the near vicinity of P the normals to W along C_{R_1} appear to converge to a point Q_1 on PN on the concave side of C_{R_1} at a distance R_1 from W. Similarly, if C_{R_2} is a line of curvature with $\rho = R_2$ at P, then in the near vicinity of P the normals to W along C_{R_2} appear to converge to a point Q_2 on PN on the concave side of C_{R_2} at a distance R_2 from W. Thus, to each point P on the wavefront W there is associated a unique pair of points Q_1 and Q_2 on the normal line PN. These points are called focal points; in general, the totality of all these points constitutes two surfaces which are called focal surfaces or caustics. These surfaces may degenerate into such forms as a single surface, a surface and a curve, a single curve, or a single point. It is important to note here that the focal surfaces are the same for all wavefronts of a particular ray congruence.

The focal surfaces can also be described in terms of the envelopes of certain families of rays. A family in this case consists of the totality of rays passing through a particular line of curvature of W, a ruled surface so constituted is known as a principal surface. Two typical families are shown in Figure 14. It is characteristic of each family that it envelopes a curve in space (S_1 and S_2 in Figure 14). It can be shown that each of these space curves lies on a focal surface;

thus, the rays of a congruence are tangent to the focal surfaces along these envelope curves. The totality of all the envelope curves constitutes the focal surfaces.

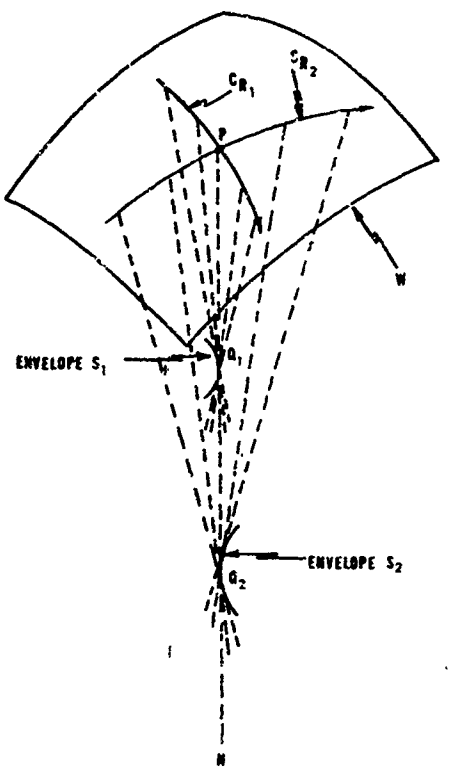

Figure 14. Ray Paths in the Principal Planes

In any specific problem regarding the determination of focal surfaces, either a ray congruence or a wavefront will generally be given. Since all wavefronts can be determined from the ray congruence and vice-versa, these two forms of the statement of the problem are entirely equivalent. In actually carrying out the computations to obtain the focal surfaces, however, the form of the statement of the problem and the functions involved will determine the best solution procedure. Two procedures will be given here—one particularly applicable when the wavefront is given and the other applicable when the ray congruence is given.

Consider the problem of determining the focal surfaces given a wavefront W in the form

$$\underset{\sim}{P} = x(u, v)\,\hat{\underset{\sim}{x}} + y(u, v)\,\hat{\underset{\sim}{y}} + z(u, v)\,\hat{\underset{\sim}{z}},$$

where $\underset{\sim}{P}$ is a vector from the origin to a point P on W and u and v are curvilinear coordinates on W. The normal vector to W at P is given by

$$\underset{\sim}{N} = \underset{\sim}{P}_u \times \underset{\sim}{P}_v,$$

where the subscripts denote partial differentiation and the expression is evaluated at P. To each of the two lines of curvature C_{R_1} and C_{R_2} through P there corresponds a principal unit normal vector. These unit vectors will be in the direction of $\underset{\sim}{N}$ or $-\underset{\sim}{N}$, whichever points to the concave side of the corresponding line of curvature. Let $\underset{\sim}{n}_1$ be the principal unit normal for C_{R_1} and let $\underset{\sim}{n}_2$ be the principal unit normal for C_{R_2}. The principal normal radii of curvature R_1 and R_2 of W at P are given by the solutions to the quadratic equation

$$(eg - f^2)\rho^2 - (Eg - 2Ff + Ge)\rho + (EG - F^2) = 0 ,$$

where

$$E = \underline{P}_u \cdot \underline{P}_u , \qquad e = (\underline{P}_{uu} \cdot \underline{N})/D ,$$

$$F = \underline{P}_u \cdot \underline{P}_v , \qquad f = (\underline{P}_{uv} \cdot \underline{N})/D ,$$

$$G = \underline{P}_v \cdot \underline{P}_v , \qquad g = (\underline{P}_{vv} \cdot \underline{N})/D ,$$

$$\text{and } D^2 = EG - F^2 = \underline{N} \cdot \underline{N} .$$

The subscripts in the above expressions denote partial differentiation. The focal points of W at P will then be given by the formulas

$$\underline{Q}_1 = \underline{P} + R_1 \underline{n}_1$$

and

$$\underline{Q}_2 = \underline{P} + R_2 \underline{n}_2 .$$

As P ranges over W, the above formulas determine the focal surfaces.

The problem of determining the focal surfaces for a given ray congruence is now considered. A ray congruence is, in general, specified by giving the ray direction at each point on a reference surface—the reference surface not necessarily being a wavefront. Let the reference surface V be given in the form

$$\underline{R} = x(u, v)\,\hat{\underline{x}} + y(u, v)\,\hat{\underline{y}} + z(u, v)\,\hat{\underline{z}} , \tag{56}$$

where $\underline{R}$ is a vector from the origin to a point R on V. Let the ray directions at each point on V be specified by the unit vector function

$$\hat{\underline{w}} = \hat{\underline{w}}(u, v) .$$

If L is the ray through R, the distances α_1 and α_2 from R along L to the focal surfaces are given by the solutions to the quadratic equation

$$(\underline{EG} - \underline{F}^2)\,\beta^2 + (\underline{Eg} - 2\underline{Ff} + \underline{Ge})\,\beta + (\underline{eg} - \underline{f}^2) = 0 . \tag{57}$$

where

$$\underline{E} = \hat{\underline{w}}_u \cdot \hat{\underline{w}}_u, \qquad e = \underline{R}_u \cdot \hat{\underline{w}}_u$$

$$\underline{F} = \hat{\underline{w}}_u \cdot \hat{\underline{w}}_v, \qquad f = \underline{R}_u \cdot \hat{\underline{w}}_v = \underline{R}_v \cdot \hat{\underline{w}}_u \tag{58}$$

$$\underline{G} = \hat{\underline{w}}_v \cdot \hat{\underline{w}}_v, \qquad g = \underline{R}_v \cdot \hat{\underline{w}}_v$$

with the subscripts denoting partial differentiation. The focal points on L will be

$$\underline{Q}_1 = \underline{R} + \beta_1 \hat{\underline{w}} \tag{59a}$$

and

$$\underline{Q}_2 = \underline{R} + \beta_2 \hat{\underline{w}} \ . \tag{59b}$$

As R ranges over V, the above formulas determine the focal surfaces.

Consider, for example, the determination of the focal surfaces or caustics produced when a paraboloid of revolution receives off-axis (Parke Mathematical Laboratories, Study No. 3, 1952). Let the paraboloid of focal length f be located with its vertex at (0, 0, f) and its focus point at the origin and let the incoming rays be in the direction

$$\hat{\underline{s}}_i = -\sin\gamma\, \hat{\underline{y}} + \cos\gamma\, \hat{\underline{z}} \ ,$$

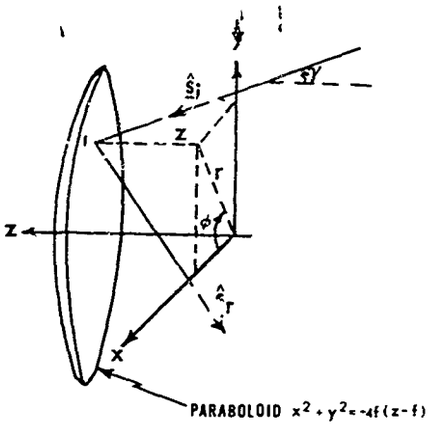

Figure 15. Geometry of Paraboloid Receiving a Plane Wave Off-Axis

as shown in Figure 15. The paraboloid surface will be considered the reference surface and in terms of the parameters r, ϕ its equation is

$$x = r\cos\phi$$

$$y = r\sin\phi$$

$$z = \frac{4f^2 - r^2}{4f} \ . \tag{60}$$

Applying Snell's law, (27c), at the reflector surface leads to the reflected ray directions

$$\underset{\sim}{s}_r = \alpha_x \underset{\sim}{\hat{x}} + \alpha_y \underset{\sim}{\hat{y}} + \alpha_z \underset{\sim}{\hat{z}} , \tag{61}$$

where

$$\alpha_x = \frac{2r^2 \sin\gamma \sin\phi\cos\phi - 4rf \cos\gamma \cos\phi}{r^2 + 4f^2}$$

$$\alpha_y = \frac{2r^2 \sin\gamma \sin^2\phi - 4rf \cos\gamma \sin\phi}{r^2 + 4f^2} - \sin\gamma \tag{62}$$

$$\alpha_z = \frac{4rf \sin\gamma \sin\phi - 8f^2 \cos^2\gamma}{r^2 + 4f^2} + \cos\gamma .$$

With

$$\underset{\sim}{R} = r\cos\phi\,\underset{\sim}{\hat{x}} + r\sin\phi\,\underset{\sim}{\hat{y}} + \frac{4f^2 - r^2}{4f}\,\underset{\sim}{\hat{z}} \text{ and } \underset{\sim}{\hat{w}} = \underset{\sim}{s}_r ,$$

the equations (60), (61), and (62) constitute a normal congruence in the usual form of a reference surface with ray directions specified at each point on the reference surface as a function of curvilinear coordinates. The second procedure for determining the focal surfaces is, therefore, the most applicable in this case.

The fundamental quantities become

$$\underline{E} = 16f^2 (\cos^2\gamma + \sin^2\gamma \sin^2\phi)/A^2$$

$$\underline{F} = (16rf^2 \sin^2\gamma \sin\phi + 8r^2 f \sin\gamma \cos\gamma \cos\phi)/A^2$$

$$\underline{G} = 4r^2 \left| r^2 + 4f^2 - (2f \sin\gamma \sin\phi + r\cos\gamma)^2 \right| /A^2$$

and

$$\underline{e} = 2(r \sin\gamma \sin\phi - 2f\cos\gamma)/A$$

$$\underline{f} = 0$$

$$\underline{g} = 2r^2(r \sin\gamma \sin\phi - 2f\cos\gamma)/A$$

where

$$A = r^2 + 4f^2 .$$

Substituting into (57) and solving for β (with much labor), we obtain

$$\beta = \frac{r^2 + 4f^2}{16f^2 (2f \cos\gamma - r \sin\gamma \sin\phi)} \left\{ \left| (r^2 - 4f^2) \sin^2\gamma + 8f^2 \right.\right.$$

$$\left. - 4rf \sin\gamma \cos\gamma \sin\phi \pm (r^2 + 4f^2) \sin\gamma \right|$$

$$\left. \sqrt{1 - \left[\frac{(r^2 - 4f^2) \cos\gamma + 4rf \sin\gamma \sin\phi}{r^2 + 4f^2} \right]^2} \right\} .$$

Equations (59a and b) then give the focal surfaces in terms of the curvilinear coordinates (r, ϕ).

In terms of cartesian coordinates (x, y, z) on the paraboloid surface, the equations for the focal surfaces become

$$\underline{Q} = \left\{ x - \frac{Bx}{2f} \right\} \underline{\hat{x}} + \left\{ y - B \left[\frac{y}{2f} + \frac{(2f - z) \sin\gamma}{2f \cos\gamma - y \sin\gamma} \right] \right\} \underline{\hat{y}}$$

$$+ \left\{ z - B \left[1 - \frac{(2f - z) \cos\gamma}{2f \cos\gamma - y \sin\gamma} \right] \right\} \underline{\hat{z}} , \qquad (63)$$

where

$$B = 2f - z + \cos\gamma (z \cos\gamma - y \sin\gamma) \pm (2f - z) \sin\gamma \sqrt{1 - \left(\frac{z \cos\gamma - y \sin\gamma}{2f - z} \right)^2} . \qquad (64)$$

Calculations for the particular case $\gamma = 20°$ have been carried out and the focal surfaces calculated and constructed (Parke Mathematical Laboratories, Report No. 1, 1952). Figures 16a, b, and c show the focal surfaces individually and superimposed.

14. GENERAL COMMENTS ON FOCAL SURFACES

The normals to a wavefront through a line of curvature tend, in general, to focus on one or the other of the two focal surfaces. The physical extent of the focal surfaces is, therefore, a measure of the focusing ability of the ray congruence associated with the wavefront. If the focal surfaces are extensive and far apart, the focusing is poor; if the focal surfaces are small and closely spaced, the focusing is good. If the focal surfaces degenerate to a line or to a point, the focusing may be considered as perfect, depending on the application.

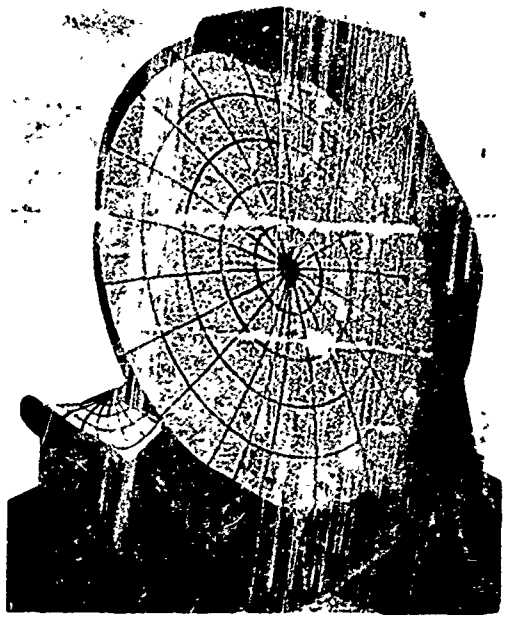

Figure 16a. Paraboloid and One Focal Surface

Figure 16b. Parapoloid and a Second Focal Surface

Figure 16c. Paraboloid and Composite of Focal Surfaces

Figure 16. Focal Surfaces of a Paraboloid Receiving a Plane Wave 20° Off-Axis

If it is desired to receive the energy of a converging wavefront by means of a point source, the optimum position for the point source will, in general, be either on one of the two focal surfaces or between them. Regions where the focal surfaces are close together or intersect generally have high energy density. Degenerate focal surfaces are also regions of high energy density. Since every ray is tangent to each of the two focal surfaces, the total energy in the wavefront can be collected by locating properly-phased receivers on one or the other or on parts of both of the focal surfaces.

For purposes of low side lobes in a focusing system there generally is a power taper across the wavefront whether considered in the focal region or in the aperture plane. This taper places greater importance on the rays through the center of a focusing system—that is, rays near the chief ray—than on rays near the edge of the system.

In general, the existence of two distinct focal surfaces in the focal region of a focusing system indicates the presence of astigmatism. For each different direction of incoming energy, the separation of the focal points Q_1 and Q_2 (see Figure 14) along the chief ray is particularly important because it is a measure of the astigmatism in a region of high power density. In most one-dimensional scanning systems, the plane of scan is a plane of symmetry of the system and also a principal surface of all ray congruences in the focal region. The other principal surfaces for all chief rays in the plane of scan will be normal to the plane of scan. As the direction of the incoming energy changes in the plane of scan, the two focal points associated with the chief ray describe two curves. Rays in the plane of scan near each chief ray will focus on one of these curves, known as the T (tangential) curve, while rays near the chief ray but in a plane normal to the plane of scan will focus on the other curve, known as the S (sagittal) curve. The separation of the S and T curves is thus a measure of the astigmatism along the chief ray for directions of incoming energy in the plane of scan and hence is an indication of the scanning capability of the system. If the S and T curves are close together, beam scanning can be accomplished by point-source feeding along a mean curve between the two. If multiple beams broad in the plane of scan but narrow in the other dimension are desired then point-source feeding along the S curve will produce the desired result. If multiple beams narrow in the plane of scan but broad in the other dimension are desired,then point-source feeding along the T curve will produce the desired result.

References

Eisenhart, L. P. (1960) A Treatise on the Differential Geometry of Curves and Surfaces, Dover Publications, New York.

Hildebrand, F. B. (1949) Advanced Calculus for Engineers, Prentice-Hall, New York, p. 294.

Holt, F. S., and Bouche, E. L. (1964) A Gregorian corrector for spherical reflectors, IEEE Trans. Antennas and Propagation, AP-12(No. 1):44-47.

Kline, M., and Kay, I. (1965) Electromagnetic theory and geometrical optics, Interscience, New York.

Kouyoumjian, R. G. (1965) Asymptotic high-frequency methods, Proc. IEEE 53:864-876.

Luneburg, R. K. (1944) Mathematical Theory of Optics, Brown University Notes, Providence, Rhode Island.

Parke Mathematical Laboratories, Inc. (1952) Calculation of the Caustic (Focal) Surface When the Reflecting Surface is a Paraboloid of Revolution and the Incoming Rays are Parallel, Study No. 3, Contract AF19(122)-484.

Parke Mathematical Laboratories, Inc. (1952) Calculation of Caustic Surface of a Paraboloid of Revolution for an Incoming Plane Wave of Twenty-Degrees Incidence, Report No. 1, Contract AF19(604)-263.

Silver, S. (1949) Microwave Antenna Theory and Design, McGraw-Hill, New York, pp. 132-134.

Sletten, C. J. et al. (1958) Corrective line sources for paraboloids, IRE Trans. PGAP AP-6(No. 3):250-251.

Spencer, R. C. (1943) Synthesis of Microwave Diffraction Patterns with Applications to $\csc^2$ Patterns, MIT Radiation Laboratory Report No. 54-24. Procedure described here due to L. J. Chu.

Appendix A

Principal Normal Radii of Curvature, Principal Directions, Principal Planes, and Lines of Curvature

Let P be a point on a surface W and let PN be a line segment normal to W at P (see Figure A1). Each normal plane through PN intersects W in a curve C and each curve C has a unique radius of curvature ρ at P. In general, for each point P there is also a unique position of the normal plane, such that the intersection curve $C = C_1$ has a radius of curvature $\rho = R_1$ at P that is maximum (see Figure A2). Similarly, there is a unique position of the normal plane, such that the the intersection curve $C = C_2$ has a radius of curvature $\rho = R_2$ that is minimum. These extreme values R_1 and R_2 are called the principal normal radii of curvature of W at P; the directions of C_1 and C_2 at P are known as the principal directions of W at P; and the normal planes whose intersect with W produce C_1 and C_2 are called the principal planes of W at P. A ve on W that at each point has a direction corresponding to a principal direction of W at that point is known as a line of curvature of W. It can be shown that the principal planes at each point are mutually orthogonal and hence the two families of lines of curvature form an orthogonal curvilinear coordinate system on W.

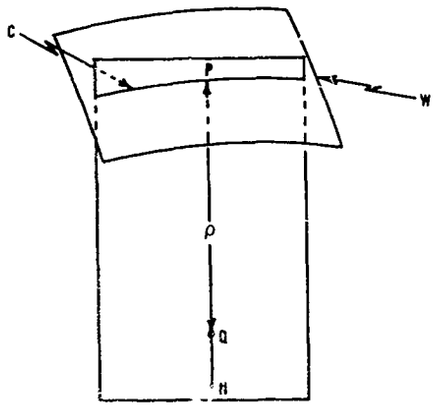

Figure A1. Surface with Normal Line and Normal Plane

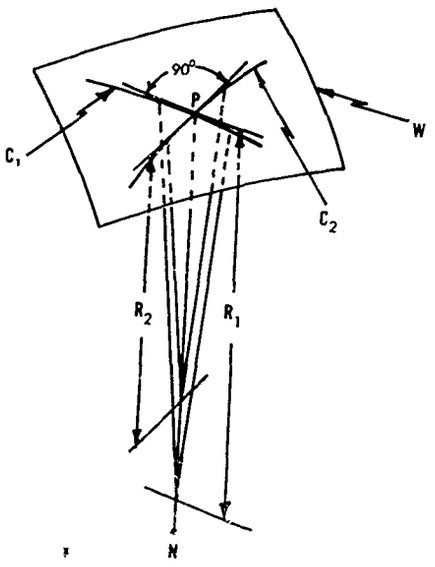

Figure A2. Principal Normal Radii of Curvature and Principal Directions at a Point on a Surface

Appendix B

Geometrical Optics Power Flow in a Source Free, Nonconducting, Isotropic, Homogeneous Medium

The ray paths for this case are straight lines (see Section 2). In Figure B1, P is a point on a wavefront W, P' is the corresponding point on the wavefront W', and d is the distance from P to P'. The differential element of area dA on W is centered at P and the corresponding element dA' is determined by the intersection of the ray tube through dA with the wavefront W'. The curves C_1 and C_2 through P are lines of curvature of W and hence are mutually orthogonal (see Appendix A). The corresponding curves C_1' and C_2' in W' are also orthogonal lines of curvature. If the principal normal radii of curvature of W at P are R_1 and R_2 and the centers of curvature are located as shown in Figure B1, the principal normal radii of curvature of W' at P' are $R_1' = R_1 + d$ and $R_2' = R_2 + d$. Thus, dA is proportional to R_1R_2 and dA' is proportional to $R_1'R_2' = (R_1+d)(R_2+d)$ If S is the power density at P and if S' is the power density at P',

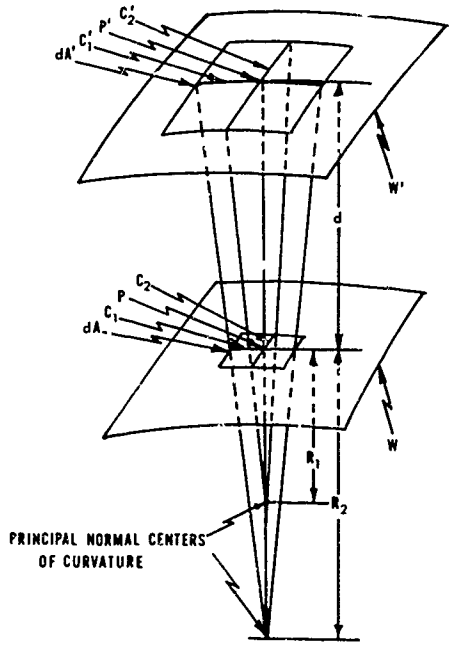

Figure B1. Geometrical Optics Power Flow

(36) becomes

$$SdA = S'dA'$$

or

$$S' = \frac{SdA}{dA'} = S\,\frac{R_1 R_2}{(R_1 + d)(R_2 + d)} . \tag{B1}$$

The Gaussian curvature K of W' at P' is defined to be

$$K = \frac{1}{R_1' R_2'} = \frac{1}{(R_1 + d)(R_2 + d)} \tag{B2}$$

and hence is a function of d . Since $K(0) = \frac{1}{R_1 R_2}$, we can write

$$S' = S\,\frac{K(d)}{K(0)} . \tag{B3}$$

This equation relates the power density S' at the point P' on a ray to the power density S at a reference point P . The power flow so expressed is equivalent to the power flow implied by the field intensity relation (26).

Unclassified
Security Classification

DOCUMENT CONTROL DATA - R&D

(Security classification of title, body of abstract and indexing annotation must be entered when the overall report is classified)

1. ORIGINATING ACTIVITY *(Corporate author)* Air Force Cambridge Research Laboratories (CRD) L. G. Hanscom Field Bedford, Massachusetts 01730	2a. REPORT SECURITY CLASSIFICATION Unclassified 2b. GROUP

3. REPORT TITLE
APPLICATION OF GEOMETRICAL OPTICS TO THE DESIGN AND ANALYSIS OF MICROWAVE ANTENNAS

4. DESCRIPTIVE NOTES *(Type of report and inclusive dates)*
Scientific. Interim.

5. AUTHOR(S) *(First name, middle initial, last name)*
F. Sheppard Holt

6. REPORT DATE September 1967	7a. TOTAL NO. OF PAGES 45	7b. NO. OF REFS 12
8a. CONTRACT OR GRANT NO.	9a. ORIGINATOR'S REPORT NUMBER(S) AFCRL-67-0501	
b. PROJECT, TASK, WORK UNIT NOS. 5635-02-01 c. DOD ELEMENT 6144501F d. DOD SUBELEMENT 681305	9b. OTHER REPORT NO(S) *(Any other numbers that may be assigned this report)* PSRP No. 340	

10. DISTRIBUTION STATEMENT
Distribution of this document is unlimited. It may be released to the Clearinghouse, Department of Commerce, for sale to the general public.

11. SUPPLEMENTARY NOTES TECH, OTHER	12. SPONSORING MILITARY ACTIVITY Air Force Cambridge Research Laboratories (CRD) L. G. Hanscom Field Bedford, Massachusetts 01730

13. ABSTRACT

The basic concepts of geometrical optics together with the additional assumption that lead to the "geometrical optics approximation" are described here. The eikonal equation is derived and the relationship of exact electromagnetic theory in the limit as $\lambda \to 0$ to geometrical optics is made evident. The application of the "geometrical optics approximation" to phase analysis and synthesis is described and an example of synthesis is presented. The concept of power flow in ray tubes is used to obtain approximations to power distributions in the antenna aperture, in the focal region, and in the far field. Ray analysis is used to determine those feed locations in the focal region that will most nearly collimate the far-field rays that lie in certain desirable planes. The Theorem of Malus is used to formulate the equal path length law and applications are given. Focal surfaces (or caustics) relative to a rectilinear congruence are defined and then used to present a geometrical optics description of the focal region. The equations of the focal surfaces of a paraboloid receiving a plane wave 20° off-axis are calculated and photographs of three-dimensional models of the focal surfaces are shown.

DD FORM 1 NOV 65 1473

Unclassified
Security Classification

Unclassified
Security Classification

14. KEY WORDS	LINK A		LINK B		LINK C	
	ROLE	WT	ROLE	WT	ROLE	WT
Microwave Optics Geometrical Optics Antenna Design and Analysis						

Unclassified
Security Classification